EAI Endorsed Transactions
on Energy Web
Research Article EAI.EU

An Ultra-Short-Term Wind Power Prediction Method Based on Quadratic Decomposition and Multi-Objective Optimization

Haoyu Chen[1,a], Zhenglong Zhang[1,b], Shaokai Tong[2,c], Peiyuan Chen[1,d], Zhiguo Wang[1,e*], Hai Huang[1,f*]

[1]College of New Energy, Xi'an Shiyou University, Xi'an 710065,

[2]Changqing Downhole Technology Company, CNPC Chuanqing Drilling Engineering Co., Ltd., Xi'an 710018, China

Abstract

To augment the accuracy, stability, and qualification rate of wind power prediction, thereby fostering the secure and economical operation of wind farms, a method predicated on quadratic decomposition and multi-objective optimization for ultra-short-term wind power prediction is proposed. Initially, the original wind power signal is decomposed using a quadratic decomposition method constituted by the Complete Ensemble Empirical Mode Decomposition with Adaptive Noise (CEEMDAN), Fuzzy Entropy (FE), and Symplectic Geometry Mode Decomposition (SGMD), thereby mitigating the randomness and volatility of the original signal. Subsequently, the decomposed signal components are introduced into the Deep Bidirectional Long Short-Term Memory (DBiLSTM) neural network for time series modeling, and the Sand Cat Swarm Optimization Algorithm (SCSO) is employed to optimize the network hyperparameters, thereby enhancing the network's predictive performance. Ultimately, a multi-objective optimization loss that accommodates accuracy, stability, and grid compliance is proposed to guide network training. Experimental results reveal that the employed quadratic decomposition method and the proposed multi-objective optimization loss can effectively bolster the model's predictive performance. Compared to other classical methods, the proposed method achieves optimal results across different seasons, thereby demonstrating robust practicality.

Keywords: wind power prediction, quadratic decomposition, multi-objective optimization, deep bidirectional long short-term memory, sand cat swarm optimization algorithm

Received on 15 November 2023, accepted on 08 April 2024, published on 15 April 2024

doi: 10.4108/ew.5787

1. Introduction

In the face of the evolving global energy structure and the escalating energy demand, wind power generation has attracted significant attention from countries worldwide, showcasing a sustained upward trajectory[1]. However, the inherent randomness and volatility of wind speed patterns pose substantial constraints on the large-scale integration of wind power generation in grid scheduling and stable operation due to natural environmental conditions[2]. Accurate forecasting of wind power significantly mitigates the uncertainty introduced by fluctuations during the integration of wind energy into the power grid. This enhancement bolsters the grid's capacity to absorb wind power, economizes the costs associated with maintaining grid stability, and elevates the efficiency of wind energy utilization.[3]. Hence, wind power prediction emerges as an area of substantial research significance in grid scheduling and stable operations.

Wind power generation is characterized by its intrinsic unpredictability and fluctuation, swayed by a plethora of meteorological elements. An in-depth comprehension of the complex liaison between meteorological observations and wind power is indispensable for enhancing the precision of wind power prognostication. Wind power prediction methodologies can be broadly bifurcated into two primary domains: physical and statistical approaches. Physical methods primarily utilize meteorological data and the

[a]23111010013@stumail.xsyu.edu.cn, [b]zhang1196438471@163.com, [c]sktong1987@126.com, [d]1427503003@qq.com
[e*]Corresponding author. Email: zhgwang@xsyu.edu.cn; [f*]huanghai@xsyu.edu.cn

operational principles of wind turbines to construct mathematical models. These models consider wind speed, wind direction, and turbine characteristics to forecast power output[4]. Li et al.[5] have championed a physical approach to wind power prediction that utilizes computational fluid dynamics to predict wind power output based on computed flow fields. Furthermore, Lin and Liu[6] have contrived an innovative blueprint for wind power prediction, amalgamating deep learning algorithms with the physical dynamics of offshore wind turbines. Their framework significantly diminishes computational overhead and prediction time while maintaining exceptional accuracy. The prediction above models enhence the precision of wind power forecasting via physical modeling; however, the intricacies involved in applying these methods and the substantial computational demands limit their widespread adoption and application.

In contrast, statistical methodologies fabricate mathematical models to elucidate the convoluted, nonlinear relationship between raw data samples and wind power output. These approaches are distinguished by their capacity to provide high precision and swift computational results[7]. Notably, deep learning algorithms have attracted considerable attention from researchers in statistical methods. Liu et al.[8] introduced a wind power prediction model that amalgamates deep learning techniques with transfer learning, demonstrating its superiority in predictive accuracy and training speed when validated against field data. In a separate study, Srivastava et al.[9] conducted a performance evaluation of recurrent neural networks, gradient boosting tree algorithms, and LSTM networks for wind power prediction, conclusively revealing the LSTM network's heightened accuracy. The experimental comparison demonstrated that the LSTM network exhibits more excellent responsiveness to high-frequency and volatile wind signals, rendering it particularly adept for modeling wind power profiles.

The optimization of hyperparameters constitutes a pivotal aspect in bolstering the predictive performance of deep learning models[7]. Manual hyperparameter tuning is a formidable task and often does not yield optimal outcomes. Hence, researchers strive to pinpoint optimal hyperparameters by deploying intelligent optimization algorithms. Wang et al.[10] utilized the particle swarm optimization algorithm to optimize pivotal parameters such as the number of time steps, hidden layer node count, and batch size in deep learning networks, thereby enhancing the predictive accuracy of natural gas price forecasts. Similarly, Liu et al.[11] optimized the learning rate of a hybrid neural network using an enhanced differential optimization algorithm, demonstrating that their proposed approach significantly bolsters the network's predictive performance and generalization capabilities.

While deep learning models have demonstrated promising results in wind power prediction, the inherent unpredictability and volatility of wind signals pose significant challenges to accurate forecasting. Signal decomposition, a technique that involves the dissection of complex signals into their constituent modal components, offers a strategy for mitigating these signals' inherent randomness and instability[12]. The application of signal decomposition algorithms for mitigating the nonlinearity in high- and low-frequency signals has garnered growing interest among researchers in time-series signal processing. For short-term photovoltaic (PV) power prediction, Liu et al.[11] integrated variational modal decomposition with an enhanced Informer model. Meanwhile, Li et al.[13] employed time-varying filter-based empirical modal decomposition (TVFEMD) to deconstruct raw data into multiple intrinsic modal function (IMF) components, subsequently incorporating sample entropy (SE) for signal reconstruction, yielding an effective prediction of the air quality index.

In summary, current wind power prediction methodologies predominantly emphasize accuracy while often overlooking stability. Ultra-short-term wind power forecasting is crucial in providing early warnings for integrating wind power into the grid, where stable and highly accurate predictions are essential for ensuring the grid's safe operation. Lu et al.[14] introduced a multi-objective optimization approach that concurrently emphasizes prediction accuracy and stability for offshore wind power prediction. The experimental results show that the multi-objective optimization approach is beneficial to improve the model's prediction accuracy. Ensuring the cost-effective operation of wind farms is paramount for rapidly advancing wind energy production. Countries worldwide have gradually established qualification standards for wind power forecasting, and any deviation from the anticipated qualification rates could potentially impose significant economic repercussions on wind farms. Consequently, this study develops a loss function for multi-objective optimization to enhance the accuracy, stability, and cost-efficiency of wind power prediction. This loss function guides the training of network models and ultimately elevates the overall performance of wind power prediction.

In the quest to enhance the precision of wind power prediction, boost grid-connection qualification rates, and guarantee the stability of such predictions, this study introduces an ultra-short-term wind power prediction methodology predicated upon quadratic decomposition and multi-objective optimization. A quadratic decomposition technique encompasses CEEMDAN, FE, and SGMD. This technique is utilized to dissect the modes inherent in the initial wind data, thereby attenuating the inherent volatility and randomness of the raw dataset. Subsequently, all the decomposed methods are integrated into the DBiLSTM neural network for time-series modeling. The DBiLSTM network is intelligently optimized by deploying the SCSO algorithm to enhance performance. Finally, a multi-objective optimization loss function is formulated, encompassing aspects of prediction accuracy, stability, and qualification rates, to guide the model training process, with the overarching aim of further facilitating the performance of the wind power prediction model.

2. Data Preprocessing

2.1. Characteristic information correlation analysis

To meticulously examine the relationship between wind power and meteorological factors, this work employs Spearman's correlation coefficient[15]. This coefficient enables a quantitative analysis of the correlation between wind power and various meteorological variables, including wind speed (at elevations of 10m, 30m, 50m, 70m), wind direction (at heights of 10m, 30m, 50m, 70m), temperature, barometric pressure, and humidity. This paper visually represents the correlation coefficients between meteorological parameters and wind power. Figure 1 displays the procured results.

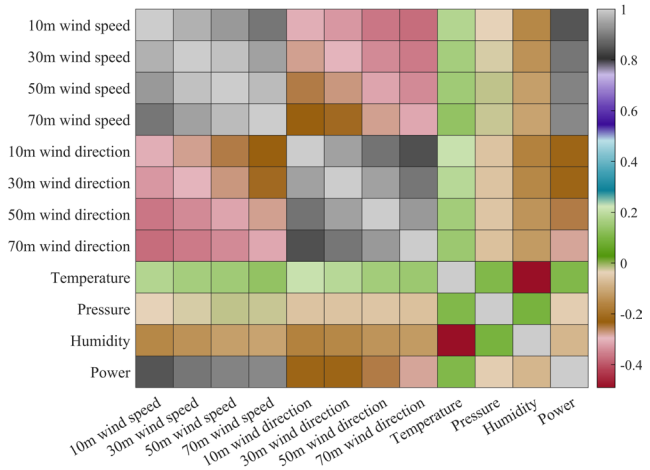

Figure 1. Spearman Correlation Coefficient Matrix

As depicted in Figure 1, the wind speed at the 70m wind measurement tower exhibits the highest correlation with wind power, at 0.9156. Therefore, this study selects the wind speed at the 70m wind measurement tower and wind power as feature inputs and normalizes both to ensure the features share the same measurement scale.

2.2. Time Lag Characterization

In this investigation, Pearson correlation coefficients are calculated between the input features and the predicted power for the initial 11 lag moments, and the outcomes are depicted in Figure 2. It merits emphasis that Li et al.[16] have proposed that correlation coefficients exceeding 0.8 signify a robust and more productive correlation in time series data, which is beneficial for feature extraction. As can be seen from Figure 2, there are nine groups with correlation coefficient values exceeding 0.8, from *t*-1 to *t*-9. Therefore, the first nine moments are selected for time series modeling.

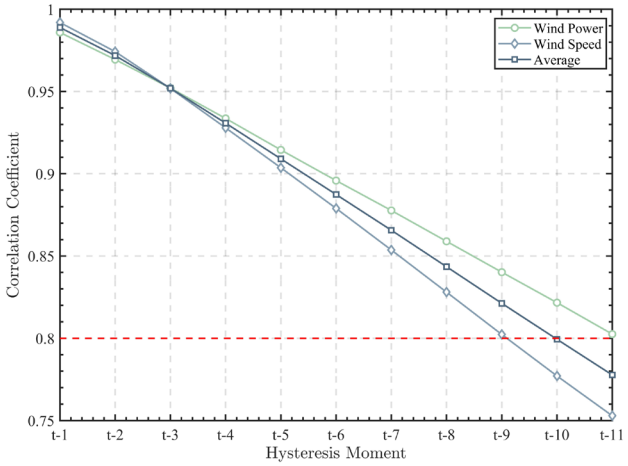

Figure 2. Pearson correlation coefficient at different times

3. Ultra-Short-Term Wind Power Prediction

3.1. Quadratic Decomposition of Wind Power Signal

This work employs a combination of quadratic decomposition and FE to tackle the variability and unpredictability inherent in wind power generation. Established signal decomposition methods encompass variational modal decomposition(VMD)[17], singular spectrum analysis(SSA)[18], and empirical modal decomposition(EMD)[19], among others. VMD needs more flexibility to select the number of components[20], which can lead to inaccurate decomposition due to either under-decomposition or modal repetition[21]. The success of SSA's decomposition hinges on the empirical selection of the window function length[22]. While EMD is a fully automated decomposition method that does not necessitate manual parameter configuration, its decomposition outcomes are susceptible to modal aliasing.

The CEEMDAN is a modal decomposition method introduced by Torres[23]. It tackles the issues of modal aliasing in empirical modal decomposition and the problem of arbitrary residual noise in aggregated empirical modal decomposition. However, various sub-components of the CEEMDAN decomposition may contain varying degrees of noise. The FE serves as a metric for quantifying each component's stochasticity, and the smoothness level for each component can be identified through FE value[24]. An appropriate FE value is used as a threshold to differentiate between non-smooth and smooth components.

The SGMD employs the symplectic geometric similarity transformation to solve and reconstruct component signals[25], effectively eliminating noise while enhancing noise robustness and adaptivity in in reconstructing component patterns[22]. Therefore, this work initially applies CEEMDAN to decompose wind power signals; subsequently,

it calculates the FE value of each sub-component, distinguishing between stationary and non-stationary components; finally, it superimposes and reconstructs the non-stationary parts, using SGMD to perform secondary decomposition on the reconstructed pieces.

Wind power and wind speed are decomposed using CEEMDAN, outputting 11 and 12 sub-components, respectively, with decomposition results shown in Figure 3 (only the first five components of wind power and wind speed are displayed). Following CEEMDAN decomposition, the nonlinearity of the signal is significantly reduced, mitigating the randomness and volatility of the original signal.

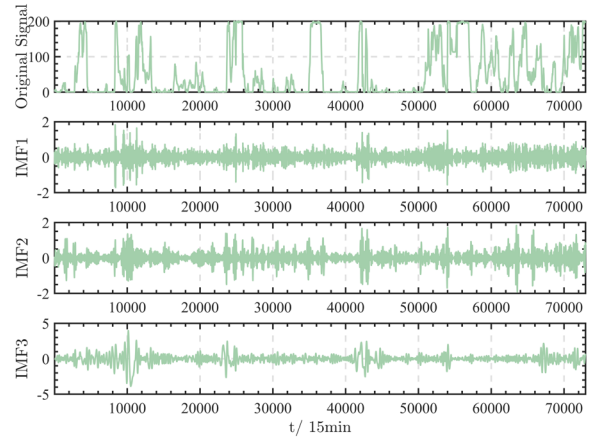

(a) Wind power component

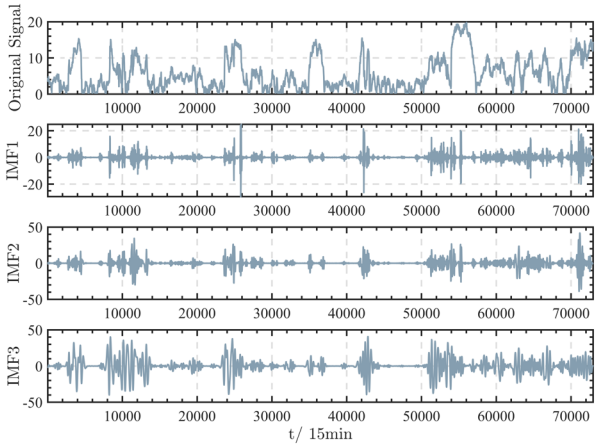

(b) Wind speed component

Figure 3. CEEMDAN decomposition result

Taking wind power as an example, the FE values for each Intrinsic Mode Function (IMF) component range from IMF1 to IMF13. The corresponding results are provided in Table 1.

As demonstrated in Table 1, the FE values of IMF1-IMF4 all surpass 0.2, markedly exceeding those of IMF5-IMF11. FE values that exceed 0.2 are indicative of non-stationary components[26]. Therefore, in this section, IMF1, IMF2, IMF3, and IMF4 are superimposed and reconstructed. The same methodology is applied to wind speed. Upon computation, the FE values of the decomposed IMF1, IMF2, and IMF3 components of the wind speed signal exceed 0.2. Therefore, superimpose and reconstruct them as well.

Table 1. FE value of 11 components

Component	FE value	Component	FE value
IMF1	0.2808	IMF7	0.0213
IMF2	0.2509	IMF8	0.0051
IMF3	0.2576	IMF9	0.0003
IMF4	0.2134	IMF10	0.00008
IMF5	0.1265	IMF11	0.00001
IMF6	0.0639		

The SGMD methodology is applied to decompose the combined components, resulting in a quadratic signal decomposition. For the reconstructed non-stationary parts of wind power and wind speed, SGMD generates 15 and 13 sub-components, respectively. Figure 4 presents the results, illustrating the first five components. Figure 4 confirms that the subsequences after secondary decomposition display improved stability and clarity.

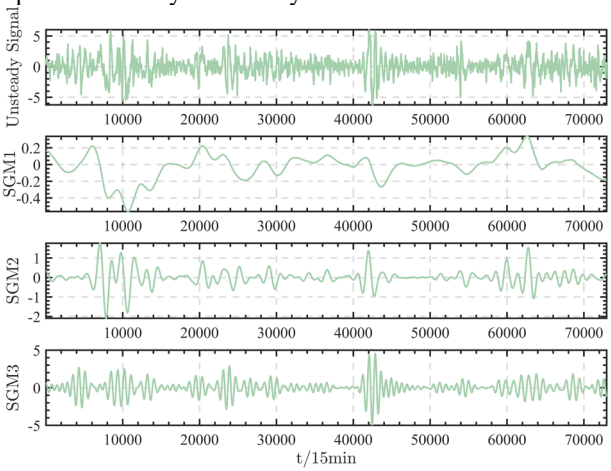

(a) Quadratic decomposition component of wind power

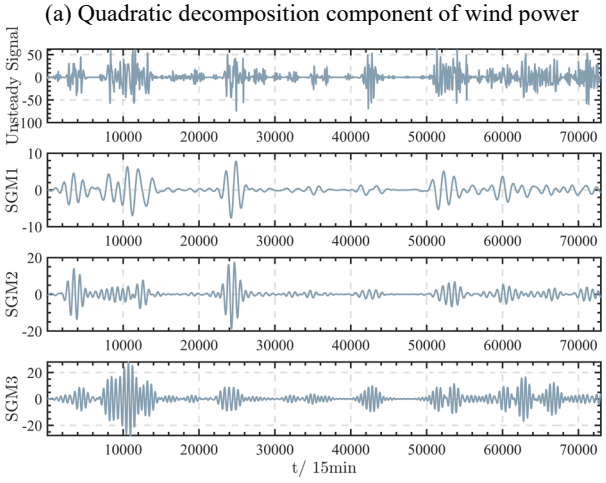

(b) Quadratic decomposition component of wind speed

Figure 4. SGMD decomposition result diagram

The raw data undergoes quadratic decomposition, producing 24 wind speed components and 25 wind power components.

3.2. DBiLSTM Timing Model Based on SCSO algorithm

The SCSO algorithm, a meta-heuristic technique, draws inspiration from the behaviour of sand cats in the wild. This algorithm is distinguished by its rapid convergence and high computational efficiency[27]. Long Short-Term Memory (LSTM) model is a prevalent method for time series prediction, which entails training a neural network to propagate the state updates of the hidden layer through unidirectional time series inputs[28]. However, in wind power prediction, where temporal dependencies span past and future time periods, conventional training methods may overlook global information embedded in historical data. Moreover, when the duration of the dataset is extended, the LSTM network may disregard the early stages of learning. To mitigate these challenges, the BiLSTM neural network is employed. This network comprises two independent LSTM networks operating at the forward and backward poles. The output of each time step is a fusion of these forward and backward LSTM networks[29]. By learning in both directions, this network is more adept at capturing valid information from historical data. Figure 5 depicts the fundamental structure of the network.

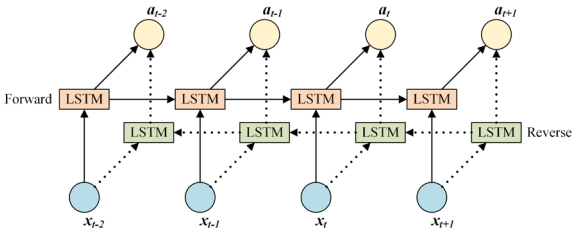

Figure 5. DBiLSTM neural network structure

The assembly of multiple layers of bidirectional long and short-term memory neural network hidden layers forms the DBiLSTM neural network. Each hidden layer integrates the forward and backward LSTM neural network outputs to generate the final result for that specific layer, as indicated in Eq. (1).

$$a_{\vartheta,t}^{join} = \left[a_{\vartheta,t}^{pos}, a_{\vartheta,t}^{rev} \right], \ \vartheta \in [1, \vartheta] \tag{1}$$

The outputs of the forward LSTM neural network, reverse LSTM neural network, and bidirectional long-short-term memory neural network in the ϑ th hidden layer at time t are denoted as $a_{\vartheta,t}^{pos}$, $a_{\vartheta,t}^{rev}$ and $a_{\vartheta,t}^{join}$, respectively. Here, ϑ represents the total number of hidden layers.

The SCSO algorithm enhances the DBiLSTM network's performance by determining the optimal number of nodes in the hidden layer and the most appropriate initial value of the network weights, thereby improving the network's prediction accuracy. Figure 6 illustrates the optimization flow of SCSO-DBiLSTM, with the specific steps detailed below:

Step 1: Inputting the quadratic decomposed wind signal into the DBiLSTM network, and the SCSO and DBiLSTM network parameters are initialized.

Step 2: The individual adjustment, $F_t = 1/L_{\text{Multi-Obj}}$, is calculated, where $L_{\text{Multi-Obj}}$ represents the test set loss of the DBiLSTM network.

Step 3: The individual position and velocity of the sand cat are adjusted.

Step 4: The termination condition is checked, i.e., whether the maximum number of iterations has been reached. If so, the optimal parameters are provided. If not, the process returns to step 2.

Step 5: The optimized parameters are incorporated into the DBiLSTM network.

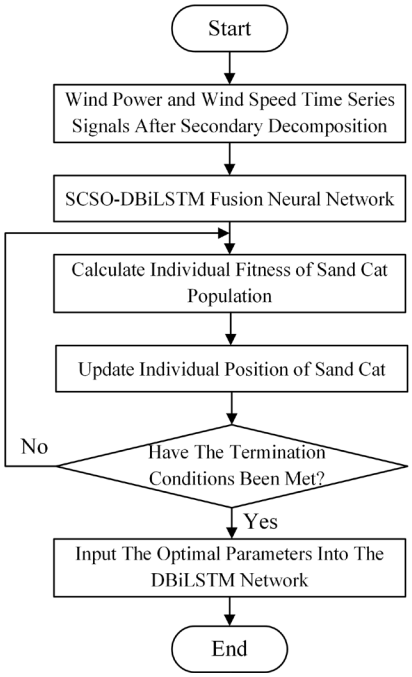

Figure 6. SCSO-DBiLSTM Optimization Flow

The SCSO-DBiLSTM network determines the number of hidden layer nodes for each BiLSTM cell through SCSO optimization. The timing modeling process is depicted in Figure 7. Initially, wind speed and power signals undergo decomposition and are then amalgamated into timing signals. These timing signals serve as the input for the SCSO-DBiLSTM network, represented as $X = [f_1, f_2, \ldots, f_n]$, where x_i symbolizes the signal obtained by the quadratic decomposition of wind speed and power at the i th moment. The SCSO-DBiLSTM network is then utilized to extract features from the input time-series signals, yielding the output feature combination $F = [f_1, f_2, \ldots, f_n]$. Finally, the feature combination F is employed for regression prediction through a fully connected layer to derive the predicted wind power. In Figure 7, the i th wind speed decomposition signal at the

moment t - k is denoted as $s_i(t - k)$, with i ranging from 1 to 25. Similarly, the j th power decomposition signal at the moment t - k is represented by p_j(t - k), with j ranging from 1 to 24. The k and n values are set to 9, as detailed in Section 1.

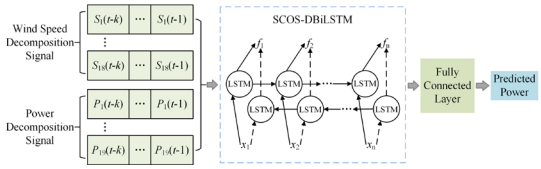

Figure 7. SCSO-DBiLSTM time series model

3.3. Ultra-short-term wind power prediction process

The framework flow of the proposed prediction method is shown in Figure 8. The specific flow is as follows:

Step 1: Input features are selected from wind power data, encompassing wind speed and historical power.

Step 2: The signals undergo CEEMDAN decomposition, yielding n signal components with distinct center frequencies.

Step 3: Calculate the decomposed components' FE values and identify non-stationary parts.

Step 4: Non-stationary components are superimposed and reconstructed before undergoing secondary decomposition via SGMD.

Step 5: The SCSO-DBiLSTM network utilizes the processed signal as input, and SCSO optimizes the number of hidden layer units in the DBiLSTM.

Step 6: Construct a multi-objective loss function optimization network and train it.

Step 7: The wind power prediction model, which has been trained, is utilized to obtain the final wind power prediction results.

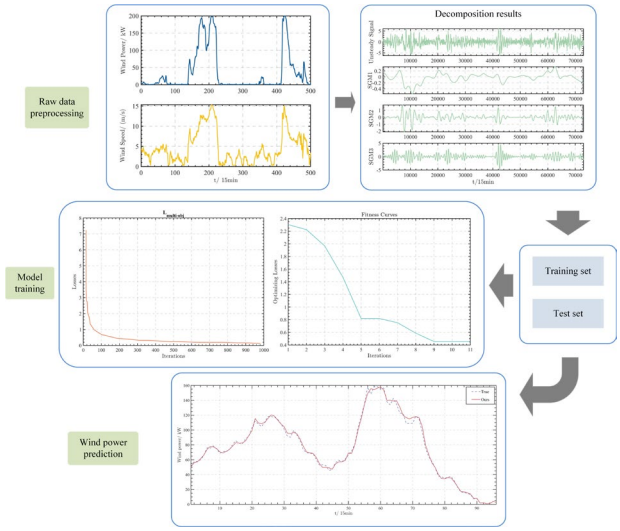

Figure 8. The framework flowchart of the proposed prediction method

3.4. Construction of the Multi-Objective Optimization Loss Function

The specific mathematical expression of the loss function designed in this work, which contains the prediction accuracy, stability, and pass rate, is given as:

$$L_1 = min\left(\frac{1}{M}\sum_{k=1}^{M}\left(\frac{p_k - y_k}{C_{cap}}\right)^2\right) \tag{2}$$

$$L_2 = min\left(\frac{1}{M-1}\sum_{k=1}^{M}\left((p_k - y_k) - E\left(P_{rediction} - Y_{true}\right)\right)^2\right) \tag{3}$$

$$r_1 = \frac{1}{M}\sum_{k=1}^{M} B_k \tag{4}$$

$$B_k = \begin{cases} 1, \left(1 - \dfrac{|p_k - y_k|}{C_{cap}}\right) \geq 0.75 \\ 0, \left(1 - \dfrac{|p_k - y_k|}{C_{cap}}\right) < 0.75 \end{cases} \tag{5}$$

$$L_3 = max\left(r_1\right) \tag{6}$$

where $P_{\text{rediction}} = \{p_k, k = 1, 2, 3, ..., M\}$ is the predicted power sample; $Y_{\text{true}} = \{y_k, k = 1, 2, 3, ..., M\}$ is the real power sample; p_k is the kth predicted power sample point. y_k is the k th real power data sample point, M is the sample capacity, C_{cap} is the total capacity of the power-on, E denotes the expectation.

L_1 and L_2 are optimization objectives for accuracy and stability, respectively. They are defined as the root mean square error and the variance between the predicted and true values of power. L_3 represents the qualified rate prediction. Accuracy, stability and pass rate are considered together in constructing the loss function. The function expression is shown in Eq. (7).

$$L = L_1 + \theta_1 L_2 + \theta_2\left(1 - L_3\right) \tag{7}$$

where θ_1 represents the weight control parameter of L_2, θ_2 represents the weight control parameter of L_3.

In the iterative process of the algorithm, the first j iterations prioritize optimizing the accuracy rate L_1, while the weights of stability L_2 and qualification rate L_3 are increased after the j iterations. The expressions for θ_1 and θ_2 are shown in Eqs. (8) and (9).

$$\theta_1(t) = min\left(\theta_{1-in}\left(1 + \theta_{1-up}\right)^{t-200}, \theta_{1-max}\right) \tag{8}$$

$$\theta_2(t) = min\left(\theta_{2-in}\left(1 + \theta_{2-up}\right)^{t-200}, \theta_{2-max}\right) \tag{9}$$

Where, t represents the number of iterations, $\theta_{1\text{-in}}$ and $\theta_{2\text{-in}}$ indicate the initial weight parameters of L_2 and L_3, $\theta_{1\text{-up}}$ and $\theta_{2\text{-up}}$ correspond to the positive factors, and $\theta_{1\text{-max}}$ and $\theta_{2\text{-max}}$ denote the maximum control coefficients of θ_1 and θ_2, respectively. The control coefficients of θ_1 and θ_2 regulate the overweighting of stability and pass rate.

4. Experimental Results and Analysis

4.1. Data Set Introduction

Taking the collected data from wind power plants in a specific region as an example, the data sampling period spans from January 1, 2017, to December 15, 2018. The sampling interval is 15 minutes, yielding 96 sample points per day over 713 days, resulting in 68,448 sample points. The 2017 data serves as the training set, while data from January 1, 2018, to December 15, 2018, constitutes the test set.

4.2. Experimental Setup

In this study, the values for θ_1 and θ_2 are fixed at 0.001, while $\theta_{1\text{-up}}$ and $\theta_{2\text{-up}}$ are set at 0.01. Additionally, $\theta_{1\text{-max}}$ and $\theta_{2\text{-max}}$ are established at 0.2. The implemented network model utilizes the Adam optimizer with a learning rate of 0.0002, a batch size of 200, and an epoch length of 1000.

4.3. Evaluation indicators

To quantitatively assess the predictive performance of different methods, we have chosen the qualification rate (QR), the mean absolute pairwise percentage error (MAPE), and the root mean square error (RMSE) as the evaluation criteria in this study. The mathematical equations are as follows:

$$MAPE = \frac{1}{M}\sum_{k=1}^{m}\left|\frac{p_k - y_k}{y_k}\right| \tag{10}$$

$$RMSE = \sqrt{\frac{1}{M}\sum_{k=1}^{M}(p_k - y_k)^2} \tag{11}$$

In the wind power prediction results, the smaller the error indicators MAPE and RMSE are, the higher the prediction accuracy is. The closer the QR is to 1, the better the model performance is.

4.4. Experimental results and analysis Ablation Experiment

The efficacy of the proposed network design was evaluated through ablation experiments on the network structure, with the results presented in Table 2. The impact of each module on performance improvement can be seen in Table 2. The intelligent optimization of hyperparameters for DBiLSTM using SCSO significantly improved network performance. Further improvements were achieved by integrating CEEMDAN signal decomposition into the SCSO-DBiLSTM framework, resulting in a 2.77% increase in QR metrics, a decrease in RMSE and MAPE to 8.568% and 1.8%, thereby underlining the substantial influence of signal decomposition. Incorporating the SGMD decomposition method led to improvements across all metrics, suggesting that quadratic decomposition of non-smooth signals based on CEEMDAN decomposition can augment model performance. The application of multi-objective optimization loss to guide network training resulted in a 76.61% improvement in QR performance and a decrease in RMSE and MAPE to 5.9385% and 11.61%, respectively. The ablation experiment underscored the effectiveness and essentiality of the proposed network structure design.

Table 2. Ablation experiment of network structure

Models	QR/%	RMSE/ %	MAPE/ %
DBiLSTM	65.37	12.3113	17.2
SCSO-DBiLSTM	68.89	10.3358	15.4
CEEMDAN + SCSO-DBiLSTM	71.66	9.4502	13.2
Secondary Decomposition + SCSO-DBiLSTM	75.45	6.7405	12.5
Secondary Decomposition + SCSO-DBiLSTM + Multi-objective Optimization	76.61	5.9385	11.61

Figure 9 depicts the wind power prediction results for various algorithm structures. The proposed model demonstrates significantly higher prediction accuracy compared to other models.

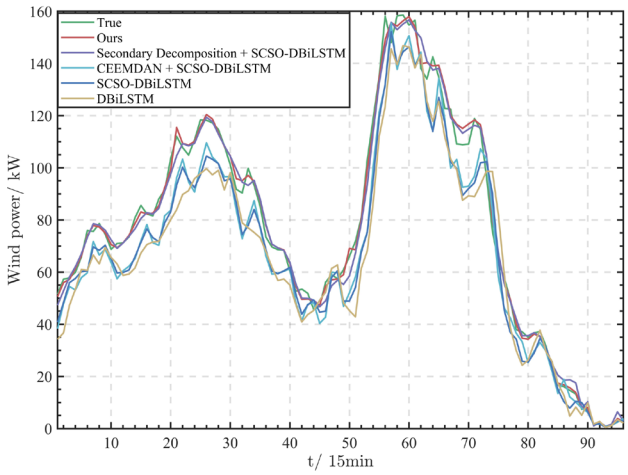

Figure 9. The framework flowchart of the proposed prediction method

Ablation experiments were further employed to assess the impact of multi-objective optimization loss on the proposed model. The results of these experiments are detailed in Table 3. The simultaneous implementation of stability and accuracy optimization losses yielded significant enhancements in the MAPE and QR. Notably, MAPE was reduced from 12.36% to 12.05%, and QR improved from 75.53% to 75.96%. The

integration of the stability loss component markedly diminished the variance of wind power prediction errors, improving the model's predictive stability and qualification rate.

Introducing the qualification rate loss to the model resulted in marked improvements across various performance metrics. Specifically, the QR improved from 75.96% to 76.61%, while the RMSE and MAPE decreased to 5.9385% and 11.61%, respectively. A comparative analysis of the ablation experiments on optimization loss reveals that incorporating multi-objective optimization loss significantly bolsters the model's accuracy, stability, and qualification rate.

Table 3. Ablation experiment of multi-objective optimalloss

Target Loss	QR/%	RMSE/%	MAPE/%
L_1	75.53	6.6536	12.36
$L_1 + \theta_1 L_2$	75.96	6.1269	12.05
$L_1 + \theta_1 L_2 + \theta_2(1 - L_3)$	76.61	5.9385	11.61

Comparison with Classical Methods

In order to fully validate the performance of wind power prediction, the proposed model is compared with Back Propagation Neural Network (BPNN)[30], LSTM[16], and Logic Gated Unit Network (GRU)[31], and the results are shown in Table 4. This table demonstrates the enhanced predictive capabilities of time series modeling methods, particularly LSTM, GRU, and our proposed approach, which exhibit lower RMSE, MAPE, and higher QR than the BPNN model. Notably, the proposed model outperforms the others across all metrics, including QR, RMSE, and MAPE.

Table 4. Performance comparison with classical algorithms

Models	QR/%	RMSE/%	MAPE/%
BPNN	52.92	18.55	37.29
LSTM	67.35	8.57	19.33
GRU	65.67	9.03.	22.04
Ours	76.61	5.9385	11.61

Figure 10 visually represents wind power prediction results over one consecutive day using various methodologies. T The graph clearly illustrates that the proposed model surpasses several alternative techniques.

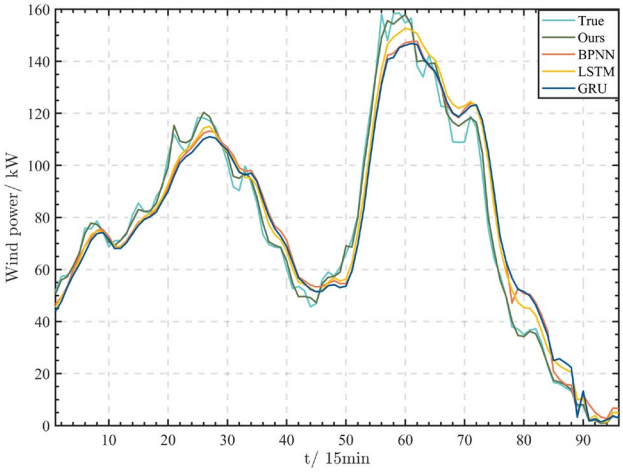

Figure 10. The framework flowchart of the proposed prediction method

Comparison of Predicted Effects for Four Seasons

To further validate the proposed model's generalization performance and take into account various seasonal wind conditions, extensive prediction comparison experiments were conducted in spring, summer, autumn and winter. The results are detailed in Table 5.

Table 5. Performance comparison between different seasons

Seasons	Model Structure	QR/%	MAPE/%	RMSE/%
Spring	BPNN	48.72	36.84	18.47
	LSTM	66.23	18.87	8.50
	GRU	63.41	21.01	8.99
	Ours	74.71	10.18	5.8755
Summer	BPNN	53.99	38.50	18.62
	LSTM	71.86	19.42	8.62
	GRU	68.17	22.45	9.10
	Ours	77.70	12.28	5.9418
Autumn	BP	51.52	37.26	18.54
	LSTM	70.07	19.36	8.59
	GRU	67.59	22.42	9.05
	Ours	76.94	11.71	5.9167
Winter	BPNN	49.55	37.11	18.57

LSTM	68.79	19.27	8.52
GRU	66.93	21.58	9.02
Ours	75.86	11.35	5.8970

Table 5 indicates that the MAPE and RMSE for various methods are typically lower in spring and higher in summer. This finding implies that the geographical location facilitates more accurate predictions in the spring, with decreased accuracy observed during summer. This variation could be due to the more stable wind speeds experienced in the area during the spring, as opposed to the more fluctuating wind speeds expected in the summer. The proposed model demonstrates superior accuracy in forecasting results for all four seasons compared to the other three methodologies.

5. Conclusion

This work proposes an ultra-short-term wind power prediction method based on CEEMDAN-FE-SGMD and multi-objective optimization to enhance prediction accuracy. The method's performance is validated using specific numerical examples. The key findings are as follows:
Incorporating a quadratic decomposition into the data reduces the randomness and volatility of the original signal, thus improving the performance of the wind prediction model. Compared to the DBiLSTM model, the QR exhibits a notable 11.24% improvement, while the MAPE and RMSE indexes decrease by 5.59% and 6.3728%, respectively. The model is trained using a multi-objective optimization loss that amalgamates accuracy, stability, and economy. The proposed method effectively reduces the model's prediction error variance, thereby enhancing both the model's strength and the grid-connection qualification rate. The optimization of the DBiLSTM network is facilitated through the SCSO algorithm, which favorably impacts the network's learning capabilities.

To validate the effectiveness of the model, three types of experiments were conducted: ablation experiments, single prediction model comparison experiments, and performance comparison experiments across different seasons. The ablation experiments' results indicate that the CEEMDAN-FE-SGMD module and the multi-objective optimization loss function module within the proposed model significantly enhance the model's prediction performance. The single prediction model comparison experiments demonstrate that the proposed method provides the most effective prediction, affirming its substantial advantage in prediction performance. Different prediction models were used to predict wind power in varying wind conditions across the four seasons. The results reveal that the proposed model exhibits the highest prediction accuracy, confirming its robust generalization performance.

The proposed methodology enhances the precision of offshore wind power prediction through multi-objective optimization, thereby improving stability and qualification rates. Nonetheless, it is critical to acknowledge that the reliability of the results is not quantifiable. Therefore, additional research in this field is necessary to evaluate and validate the dependability of the methodology thoroughly.

Acknowledgements.

The authors would wish to acknowledge the support of the QinetiQ's "Scientists + Engineers" programme (grant number 2023KXJ-172). This work was also supported by the Youth Innovation Team of Shaanxi Universities.

References

[1] N. Kumar, O. Prakash, Analysis of wind energy resources from high rise building for micro wind turbine: A review, Wind Engineering. 47 (2023) 190–219.
[2] W. Jiang, B. Liu, Y. Liang, H. Gao, P. Lin, D. Zhang, G. Hu, Applicability analysis of transformer to wind speed forecasting by a novel deep learning framework with multiple atmospheric variables, Applied Energy. 353 (2024) 122155.
[3] Z. Yang, W. Huang, S. Dong, H. Li, Mixture bivariate distribution of wind speed and air density for wind energy assessment, Energy Conversion and Management. 276 (2023) 116540.
[4] G. Yu, C. Liu, B. Tang, R. Chen, L. Lu, C. Cui, Y. Hu, L. Shen, S.M. Muyeen, Short term wind power prediction for regional wind farms based on spatial-temporal characteristic distribution, Renewable Energy. 199 (2022) 599–612.
[5] L. Li, Y. Liu, Y. Yang, S. Han, Y. Wang, A physical approach of the short-term wind power prediction based on CFD pre-calculated flow fields, J Hydrodyn. 25 (2013) 56–61.
[6] Z. Lin, X. Liu, Wind power forecasting of an offshore wind turbine based on high-frequency SCADA data and deep learning neural network, Energy. 201 (2020) 117693.
[7] M. Neshat, M.M. Nezhad, E. Abbasnejad, S. Mirjalili, L.B. Tjernberg, D. Astiaso Garcia, B. Alexander, M. Wagner, A deep learning-based evolutionary model for short-term wind speed forecasting: A case study of the Lillgrund offshore wind farm, Energy Conversion and Management. 236 (2021) 114002.
[8] X. Liu, Z. Cao, Z. Zhang, Short-term predictions of multiple wind turbine power outputs based on deep neural networks with transfer learning, Energy. 217 (2021) 119356.
[9] T. Srivastava, Vedanshu, M.M. Tripathi, Predictive analysis of RNN, GBM and LSTM network for short-term wind power forecasting, Journal of Statistics and Management Systems. 23 (2020) 33–47.
[10] J. Wang, J. Cao, S. Yuan, M. Cheng, Short-term forecasting of natural gas prices by using a novel hybrid method based on a combination of the CEEMDAN-SE-and the PSO-ALS-optimized GRU network, Energy. 233 (2021) 121082.
[11] L. Liu, J. Wang, J. Li, L. Wei, Monthly wind distribution prediction based on nonparametric estimation and modified differential evolution optimization algorithm, Renewable Energy. 217 (2023) 119099.
[12] X. He, X. Zhou, J. Li, C.K. Mechefske, R. Wang, G. Yao, Q. Liu, Adaptive feature mode decomposition: a fault-oriented vibration signal decomposition method for identification of multiple localized faults in rotating machinery, Nonlinear Dyn. 111 (2023) 16237–16270.
[13] Y. Li, T. Peng, L. Hua, C. Ji, H. Ma, M.S. Nazir, C. Zhang, Research and application of an evolutionary deep learning

model based on improved grey wolf optimization algorithm and DBN-ELM for AQI prediction, Sustainable Cities and Society. 87 (2022) 104209.
[14] H. Lu, X. Ma, K. Huang, M. Azimi, Prediction of offshore wind farm power using a novel two-stage model combining kernel-based nonlinear extension of the Arps decline model with a multi-objective grey wolf optimizer, Renewable and Sustainable Energy Reviews. 127 (2020) 109856.
[15] Z. Cao, J. Wang, L. Yin, D. Wei, Y. Xiao, A hybrid electricity load prediction system based on weighted fuzzy time series and multi-objective differential evolution, Applied Soft Computing. 149 (2023) 111007.
[16] J. Li, D. Geng, P. Zhang, X. Meng, Z. Liang, G. Fan, Ultra-Short Term Wind Power Forecasting Based on LSTM Neural Network, in: 2019 IEEE 3rd International Electrical and Energy Conference (CIEEC), IEEE, Beijing, China, 2019: pp. 1815–1818.
[17] D. Zosso, K. Dragomiretskiy, Variational Mode Decomposition, IEEE Transactions on Signal Processing: A Publication of the IEEE Signal Processing Society. (2014).
[18] R. Vautard, P. Yiou, M. Ghil, Singular-spectrum analysis: A toolkit for short, noisy chaotic signals, Physica D: Nonlinear Phenomena. 58 (1992) 95–126.
[19] H. Ne., L. Sr., W. Mlc., S. Hh., Z. Qn., Y. Nc., T. Cc., L. Hh., Z. Shen, The empirical mode decomposition and the Hilbert spectrum for nonlinear and non-stationary time series analysis, Proceedings of the Royal Society. Mathematical, Physical and Engineering Sciences. (1998) 454.
[20] D. Li, F. Jiang, M. Chen, T. Qian, Multi-step-ahead wind speed forecasting based on a hybrid decomposition method and temporal convolutional networks, Energy. 238 (2022) 121981.
[21] S. Parri, K. Teeparthi, V. Kosana, A hybrid VMD based contextual feature representation approach for wind speed forecasting, Renewable Energy. 219 (2023) 119391.
[22] X. Zhang, C. Li, X. Wang, H. Wu, A novel fault diagnosis procedure based on improved symplectic geometry mode decomposition and optimized SVM, Measurement. 173 (2021) 108644.
[23] M.E. Torres, M.A. Colominas, G. Schlotthauer, P. Flandrin, A complete ensemble empirical mode decomposition with adaptive noise, in: 2011 IEEE International Conference on Acoustics, Speech and Signal Processing (ICASSP), IEEE, Prague, Czech Republic, 2011: pp. 4144–4147.
[24] H. Zhou, W. Chen, C. Shen, L. Cheng, M. Xia, Intelligent machine fault diagnosis with effective denoising using EEMD-ICA- FuzzyEn and CNN, International Journal of Production Research. 61 (2023) 8252–8264.
[25] H. Pan, Y. Yang, X. Li, J. Zheng, J. Cheng, Symplectic geometry mode decomposition and its application to rotating machinery compound fault diagnosis, Mechanical Systems and Signal Processing. 114 (2019) 189–211.
[26] Y. Wang, D. Wang, Investigations on sample entropy and fuzzy entropy for machine condition monitoring: revisited, Meas. Sci. Technol. 34 (2023) 125104.
[27] A. Seyyedabbasi, F. Kiani, Sand Cat swarm optimization: a nature-inspired algorithm to solve global optimization problems, Engineering with Computers. 39 (2023) 2627–2651.
[28] S. Ray, A. Lama, P. Mishra, T. Biswas, S. Sankar Das, B. Gurung, An ARIMA-LSTM model for predicting volatile agricultural price series with random forest technique, Applied Soft Computing. 149 (2023) 110939.
[29] Y. Song, H. Xie, Z. Zhu, R. Ji, Predicting energy consumption of chiller plant using WOA-BiLSTM hybrid prediction model: A case study for a hospital building, Energy and Buildings. 300 (2023) 113642.
[30] J. Liu, X. Wang, Y. Lu, A novel hybrid methodology for short-term wind power forecasting based on adaptive neuro-fuzzy inference system, Renewable Energy. 103 (2017) 620–629.
[31] A. Kisvari, Z. Lin, X. Liu, Wind power forecasting – A data-driven method along with gated recurrent neural network, Renewable Energy. 163 (2021) 1895–1909.